Received: 10 April 2019 | Revised: 3 February 2020 | Accepted: 10 February 2020

DOI: 10.1002/ldr.3577

WILEY

RESEARCH ARTICLE

Remote sensing estimation of the soil erosion cover-management factor for China's Loess Plateau

Xihua Yang[1,2,3] | Xiaoping Zhang[1] | Du Lv[1] | Shuiqing Yin[4] | Mingxi Zhang[2,3] | Qinggaozi Zhu[5] | Qiang Yu[1,2] | Baoyuan Liu[1,4]

[1]State Key Laboratory of Soil Erosion and Dryland Farming on the Loess Plateau, Institute of Soil and Water Conservation, Northwest A & F University, Yangling, Shaanxi, PR China

[2]School of Life Sciences, Faculty of Science, University of Technology, Sydney, Australia

[3]New South Wales Department of Planning, Industry and Environment, Parramatta, New South Wales, Australia

[4]School of Geography, Beijing Normal University, Beijing, PR China

[5]New South Wales Department of Primary Industry, Parramatta, New South Wales, Australia

Correspondence
Xiaoping Zhang, State Key Laboratory of Soil Erosion and Dryland Farming on the Loess Plateau, Institute of Soil and Water Conservation, Northwest A & F University, Yangling, Shaanxi 712100, PR China.
Email: zhangxp@ms.iswc.ac.cn

Funding information
State Key Laboratory of Soil Erosion and Dryland Farming on the Loess Plateau, Grant/Award Number: A314021403-1703; National Natural Science Foundation of China, Grant/Award Number: 41877083

Abstract

The cover-management factor (C-factor) is used in the revised universal soil loss equation to represent the effect of vegetation cover and its management practices on hillslope erosion. Remote sensing has been widely used to estimate vegetation cover and the C-factor, but most previous studies only used the photosynthetic vegetation (PV) or green vegetation indices (VI, e.g., normalized difference VI) for estimating the C-factor and the important non-PV (NPV) component was often ignored. In this study, we developed a new technique to estimate monthly time-series C-factor using the fractional vegetation cover (FVC) including both PV and NPV, and weighted by monthly rainfall erosivity ratio. The monthly FVC was derived from the moderate resolution imaging spectroradiometer and LANDSAT data with field validation. We conducted the case-study over China's Loess Plateau and analysed the spatiotemporal variations of FVC and the C-factor and their impacts on erosion over the Plateau. Our study reveals a significant increase in total vegetation cover (TC) from 56 to 76.8%, with a mean of 71.2%, resulting in about 20% decrease in the C-factor and erosion risk during the 17-year period. Our method has an advantage in estimating the C-factor from TC at a monthly scale providing a basis for continuously and consistently monitoring of vegetation cover, erosion risk and climate impacts.

KEYWORDS

cover-management factor, fractional vegetation cover, land degradation, Loess Plateau, remote sensing, soil erosion, time series

1 | INTRODUCTION

Land degradation driven by accelerated soil erosion is a widespread issue and the situation will continue during the 21st century, especially in developing countries of the tropics and subtropics (Lal, 2001). Soil erosion removes fertile topsoil that contains most of the soil's plant nutrients and soil microorganisms that contribute to soil health, which leads to a loss of soil productivity and biodiversity. The subsequent increase in sediment deposition and nutrient enrichment may cause environment and water quality degradation in rivers, lakes and reservoirs (e.g., Borrelli et al., 2018).

Soil erosion is often associated with reduction of vegetative cover (both living and dead) of soil surfaces due to inappropriate land management practices, extreme climate variability (e.g., storm events) and natural hazards (e.g., wildfires). The primary human-controlled drivers on vegetation are, for example, animal stocking rate for grazing lands and tillage and other forms of management of plant residues for cropping lands (Cao, Li, Liu, Chen, & Wang, 2018). Land management practices are particularly important in erosion control in a semiarid environment such as China's Loess Plateau.

The revised universal soil loss equation (RUSLE) defines a cover and management factor (C-factor) to reflect the effect of cropping and management practices on erosion rates. The C-factor indicates

how the concerned vegetation cover type will affect the average annual soil loss and how that soil-loss potential will be affected in time by land management practices such as crop rotations or forest plantation (Wischmeier & Smith, 1978). For the C-factor in a certain period during a year such as crop growing period or a month, the erosion control effectiveness also depends on how the annual erosive rainfall is distributed in that specific period (Renard, Foster, Weesies, McCool, & Yoder, 1997).

It can be complex to evaluate and parameterise the effect of actual vegetation cover and management practices on soil erosion. The alternative method in RUSLE is to use the empirical relationships of soil loss and the subfactors including the previous land use (PLU), canopy cover (CC), surface cover (SC), surface roughness (SR) and soil moisture (SM) to estimate soil loss ratios (SLR) which is defined as the ratio of soil loss under actual conditions to losses experienced under the reference conditions (Renard et al., 1997). These subfactors should be estimated for each time period of the year over which the single subfactors can be assumed to remain constant, considering the seasonal variations due to crop rotation or other natural effects (climate variability, plant health conditions, etc.). Although this procedure is rather onerous and complicated, a suitable SLR relationship with ground vegetation cover provides a practical means to estimate the C-factor over large areal extents, especially when incorporated with remotely sensed data (Benkobi et al., 1994). The C-factor value is an average SLR weighted according to the distribution of rainfall erosivity (R-factor) during the year, thus SLR and the C-factor is the same on an annual basis. The R-factor ratio needs to be used to redistribute SLR to a specific subperiod. On a monthly basis, for example, the C-factor is estimated by the SLR multiplied by the rainfall erosivity ratio at that month.

Remote sensing has been used to estimate the C-factor by means of land cover classifications, vegetation indices (VI), or a combination of these (Feng & Zhao, 2014; Li & Gao, 2016; Panagos et al., 2015). In most studies, VI values are directly converted to the C-factor values by a linear or an exponential regression. Correlation analysis has been used to construct the relationships between the normalized difference VI (NDVI) from remote sense imagery and the C values from lookup tables (De Asis & Omasa, 2007; Wang, Wente, Gertner, & Anderson, 2010). However, the correlation was quite low (Puente et al., 2011; Yang, 2014) because NDVI is merely focused on green vegetation or photosynthetic vegetation (PV) without consideration of nongreen or non-PV (NPV) which can also significantly influence the SLR and the C-factor (Vatandaşlar & Yavuz, 2017; Vrieling, 2006). Ignoring the NPV component often results in misleading declaration and incorrect conclusions as the findings do not correctly represent the true fraction of vegetation cover that protects soil from erosion (De Asis & Omasa, 2007; De Jong, 1994; Tanyaş, Kolat, & Süzen, 2015). It appears to be necessary to use an FVC index instead of NDVI as the earlier can better reflect the vegetation composition (Ko, Kim, Narantsetseg, & Kang, 2017; McKenzie et al., 2017). However, there is a significant knowledge gap in remote sensing of NPV and incorporating the information of NPV and ground litter into the C-factor estimation (Song et al., 2017). Yang (2014) first attempted using the FVC products (PV and NPV) to estimate the C-factor over New South Wales (NSW), Australia and the methods were primarily applicable for pasture or natural environment in Australia. Such FVC indices and the relationships with the RUSLE C-factor need to be further explored over different regions and landscapes.

Therefore, the objective of this study was to develop a new and practical approach to estimate the SLR and the C-factor values for soil erosion modelling at monthly interval from the emerging satellite-based FVC products including PV, NPV and bare soil (BS), with weighting of rainfall erosivity ratio as per RUSLE guideline. The specific aims were to: (a) estimate and map monthly and annual C-factor over the entire Loess Plateau using FVC; (b) compare and cross validate FVC and C-factor values derived from moderate resolution imaging spectroradiometer and LANDSAT; (c) analyse the spatiotemporal changes of FVC and the C-factor and (d) identify the areas with potential erosion risk (or the likelihood) across the Loess Plateau and the main drivers. As the time-series FVC data sets are now available globally, the methodology developed in this study is expected to be applicable anywhere in the world in C-factor estimation and soil erosion modelling.

2 | THE CASE STUDY AREA, CHINA'S LOESS PLATEAU

We chose China's Loess Plateau as the case study area for these three reasons: (a) it's one of the worst areas subject to land degradation in the world; (b) it experienced the significant changes in vegetation cover and (c) there are a lot of relevant studies on soil erosion, remote sensing and vegetation.

The Loess Plateau region covers an area of approximately 624,000 km^2 (83% of the Yellow River Catchment) located in the highland area in north-central China. It covers northern Shaanxi and Henan, much of Shanxi, eastern Gansu and Ningxia and southern Inner Mongolia (Figure 1).

The Loess Plateau has a continental monsoon climate with a mean temperature of 9.1°C and mean annual precipitation 460 mm (1980–2010), 65% of which occurs between July and September with high intensity (Jin, Zhang, Shi, & Huang, 2016). The loess soil, equivalent to Calcic Cambisol in the World Soil Reference Base System (IUSS Working Group WRB, 2014), dominates this region and it is highly erodible. The ground water table depth ranges from 50 to 200 m, thus growth and survival of vegetation rely on the availability of water from precipitation (Jian, Zhao, Fang, & Kai, 2015). Agricultural activities normally take place in the alluvial plain and the flat areas.

The dominant landforms of the region are the so-called Hilly gully landscape in the southern and central areas, and the sandy desert in the western and northern part, accounting for 58 and 42%, respectively (Yang & Yuan, 1991). The average slope is approximately 24% with steep slope (>25%) accounting for about 38% of the total area. The altitude of the Loess Plateau ranges from 800 to 3,000 m with the relative relief of 100 to 300 m in most areas. The landscape is

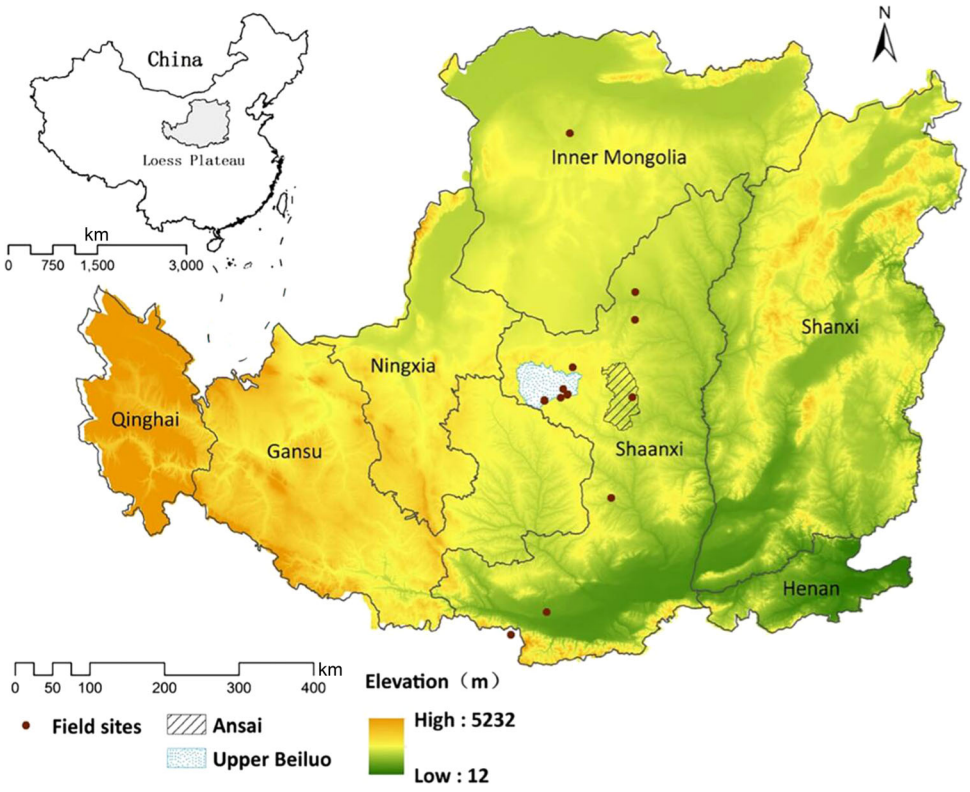

FIGURE 1 The study area and locations of previous research areas and field measurement sites over the Loess Plateau of China [Colour figure can be viewed at wileyonlinelibrary.com]

heavily dissected with the gully density up to 8 km km^{-2}. The Loess Plateau is characterised by severe soil erosion with the average erosion rate from 50 to 100 Mg ha^{-1} year^{-1}. It is believed that intensive human activities such as deforestation and inappropriate land use practices with rapid population growth over an extended period of time have caused the land degradation and severe soil loss (Yang & Yuan, 1991). The concentrated and high-intensity rainfall, high soil erodibility and sparse vegetation cover combined with the heavily dissected landscape, all contribute significantly to the severe erosion and consequent land degradation (Chen et al., 2018).

As key practices of soil and water conservation, afforestation and pasture improvement has been continuously implemented over the Loess Plateau since the 1950s. The program of 'Grain for Green' (GFG) Programme was launched by the Government in 1999 across the whole Plateau, especially in the areas subject to land degradation. The aim was to convert the slope farmland to forest and grassland to improve vegetation cover, control soil erosion and foster soil quality. Recent research has shown that the vegetation cover has greatly improved since 1999 (Zhang et al., 2018). Since then, there have been a lot of studies on soil erosion and vegetation over the Loess Plateau. Recent studies on China's Loess Plateau reemphases that the C-factor is more sensitive to nongreen vegetation or NPV, and highlights that the NPV and litter cannot be ignored (Feng, Zhao, Ding, Fang, & Zhang, 2017). In comparisons among the six VIs, it has been found that the normalized difference senescent VI (NDSVI) (Qi et al., 2002) has the highest correlation with the C-factor values in relation to a single VI over the Loess Plateau (Feng et al., 2017; Zhao, Fu, & Chen, 2012). However, most of the existing studies on the C-factor estimation do not consider the NPV component (Zhang, Hu, & Shi, 2016) and the temporal variations of vegetation cover and management, nor do they take rainfall erosivity into account in the C-factor calculation (Zhao, Fu, & Qiu, 2013). Monthly time-series estimates of the C-factor as per RUSLE guideline (Renard et al., 1997) have never been done over the Loess Plateau for extended periods.

3 | METHODS

3.1 | Datasets

The dominant datasets used in this study include MODIS derived FVC, LANDSAT (5, 7 and 8) images and digital elevation models (DEMs), as well as some ancillary datasets including land use, rainfall, soil, field data and relevant outcomes from previous research. The major datasets are briefly described below.

MODIS-based FVCs were estimated from MODIS data (MCD43A4, MOD09A1) and the methodology is described in Guerschman et al. (2009). The recent global FVC products include monthly fractional cover (percentage) of PV, NPV aological Survey (USGSnd BS at a spatial resolution of 500 m. The FVC products have gone through several improvements with user feedback and field measurements from thousands of field sites (Guerschman et al., 2015). The current version is V3.1.0 and the reported root mean square errors (RMSE) are 0.112, 0.162 and 0.130 for PV, NPV and BS, respectively (Chappell et al., 2017; Guerschman & Hill, 2018). The time-series FVC products are now available free globally through the

Global Agricultural Monitoring (GEOGLAM) initiative (Evans, Antony, Guerschman, Larraondo, & Richards, 2017).

All 'cloud-free' (< 10%) LANDSAT (5, 7 and 8) images (13,801 scenes in total) within the Loess Plateau area have been collected from the US Geological Survey (USGS) LANDSAT data archive (https://earthexplorer.usgs.gov/) for the period 2001–2017. Such large quantity LANDSAT data were processed using the Google Earth Engine (GEE) platform.

The Shuttle Radar Topography Mission (SRTM) derived DEMs at 30 m were downloaded from the USGS via the Earthexplorer web site (https://earthexplorer.usgs.gov) and used for calculation of the slope-steepness factor (LS-factor) as described in Yang (2015). Monthly and annual rainfall erosivity was calculated from daily precipitation data based on Xie, Yin, Liu, Nearing, & Zhao (2016) using all available rain gauge data in the study area. The monthly rainfall erosivity data were further used to calculate monthly distribution of the C-factor.

We also collected relevant data from previous studies at central Loess Plateau (Wuqi and Ansai County, refer Figure 1) for comparison and validation purposes. Monthly SLR data for major crop types were obtained from published research findings (Feng et al., 2017; Zhao et al., 2012; Zhao et al., 2013). Their research also produced major land use/cover types including farmland, forestland, shrubland, woodland, grassland, water bodies and built-up land (Fu et al., 2005; Zhao et al., 2013), as well as the 30 m global land cover products from China (Gong et al., 2013). The land use/cover data and the impacts on runoff and erosion were further analysed by Zhang et al. (2018) and their findings provided good comparison to this study.

In addition, we carried 81 field measurements on selected sites at Upper Beiluo Catchment (UBC) and along a South–North transect approximately 700 km with different land uses (refer Figure 1) since 2015 to measure FVC and spectral reflectances at different seasons which were in turn used to validate the remotely sensed FVC and the related VI used to estimate the FVC (see Section 3.5 for details).

3.2 | Remote sensing of fractional vegetation cover

The methods and products of MODIS derived FVC are well described in Guerschman et al. (2009) and updated using the new Nadir BRDF-Adjusted Reflectance Collection 6 reflectance product and a major expansion of the field calibration database (Guerschman & Hill, 2018). They kindly supplied the FVC products (PV, NPV BS) for our pilot study on the Loess Plateau and the global data sets are now available through GEOGLAM RAPP (https://map.geo-rapp.org/). We further processed the monthly FVC products to fill the gaps (due to clouds or no data) and correct abnormal data by using specific spatial masks (e.g., water, snow, urban, conservation areas) before they were used to estimated C-factor. MODIS vegetation (NDVI) indices products (MOD13Q1) were used to estimate the FVC for these gaps based on the correlation between NDVI and FVC on monthly basis. Specific C-factor values were assigned to nonvegetation groundcover types such as water (C = 0.0001), snow (C = 0.0044) and urban built-up areas (C = 0.0039). Automated scripts in geographic information system (GIS) were developed for these gap-filling processes. The total vegetation cover (TC) from MODIS derived FVC was calculated by summing PV and NPV percentages.

In addition to the MODIS derived FVC products, we also estimated the FVC from LANDSAT imagery and used to compare with the MODIS estimation or cross-validation. For LANDSAT-based estimation, the PV fraction (fPV) was estimated using the modified transformed VI (MTVI) (Haboudane, Miller, Pattey, Zarco-Tejada, & Strachan, 2004; Smith, Hill, & Zhang, 2015; Zhang & Smith, 2010) using the near infrared (NIR) and the visible bands:

$$f\mathrm{PV} = 1.7208[1.2(R_{\mathrm{NIR}} - R_{\mathrm{green}}) - 2.5(R_{\mathrm{red}} - R_{\mathrm{green}})] + 0.1004 \quad (1)$$

The non-PV fraction (fNPV) was estimated from the NDSVI (Qi et al., 2002) as it has the highest correlation with the C-factor values in relation to a single VI over the Loess Plateau (Feng et al., 2017; Zhao et al., 2012). The NDSVI is based on a combination of red (i.e., TM3 or OLI4) and shortwave infrared (SWIR, i.e., TM5 or OLI5) reflectance from LANDSAT imagery showed good sensitivity to NPV cover as NPV scattering mostly occurs in the SWIR ranges (Marsett et al., 2006; Zhang & Smith, 2010):

$$\mathrm{NDSVI} = (R_{\mathrm{SWIR}} - R_{\mathrm{red}})/(R_{\mathrm{SWIR}} + R_{\mathrm{red}}) \quad (2)$$

$$f\mathrm{NPV} = 0.82\,\mathrm{NDSVI} + 0.0753 \quad (3)$$

The TC from LANDSAT was calculated as the summary of fPV and fNPV percentages derived as above:

$$\mathrm{TC} = f\mathrm{PV} + f\mathrm{NPV} \quad (4)$$

In Equations (1) and (2), R indicates reflectance values and the subscripts are the wavelengths or bands. The corresponding image bands for Green, Red, NIR and SWIR are 2–5 for LANDSAT Thematic Mapper (TM, LANDSAT 5 and 7) and 3–6 for Operational Land Imager (OLI, LANDSAT 8), respectively.

3.3 | The C-factor estimation

In the RUSLE, SLR is calculated as the product of five subfactors:

$$\mathrm{SLR} = \mathrm{PLU} \times \mathrm{CC} \times \mathrm{SC} \times \mathrm{SR} \times \mathrm{SM} \quad (5)$$

where PLU is the prior-land use, CC is the canopy cover, SC is the surface cover, SR is the surface roughness and SM is the soil moisture.

An exponential function of SLR and vegetation cover based on the plot experiments was developed and validated over the Loess Plateau by Jiang, Wang, and Liu (1996), which is considered suitable for this study area (Zhang, Yuan, & Liu, 2002) and the similar approach has also been applied elsewhere (e.g., Yang, 2014). In consideration of

the distribution of monthly rainfall erosivity, the monthly SLR (SLR_i) and the C-factor (C_i), and the annual C-factor (C) were estimated using the following equations.

$$SLR_i = e^{-0.0418(TC_i - 5)} \quad (6)$$

$$C_i = SLR_i \times EI_i / EI_t \quad (7)$$

$$C = \sum_{i=1}^{12} C_i \quad (8)$$

where SLR_i is the SLR in month i (1–12), TC_i is the total percentage of ground cover (0–100) or TC (PV + NPV) in that month estimated from Equation (4), C_i is the monthly cover-management factor in month i, EI_i is the monthly rainfall erosivity in that month, EI_t is the total rainfall erosivity in the year. The sum of monthly C_i (12 months) is the annual cover and management factor (C). When the ground cover is less than 5% (e.g., BS), the SLR value is regarded as 1.0 over the Loess Plateau, and when the ground cover is greater than 5%, Equations (6)–(8) are applied to estimate C.

The monthly (EI_i) and annual rainfall erosivity (EI_t) was estimated from daily rainfall records at 91 meteorological stations across the Plateau by using a daily rainfall erosivity model and a Kriging interpolation method as described in Xie, Yin, Liu, Nearing, and Zhao (2016).

$$R_{day} = \alpha {P_d}^{1.7265} \; (P_d > 10\,\text{mm}) \quad (9)$$

where R_{day} is the daily rainfall erosivity, P_d is the daily rainfall amount (>10 mm, small rainfall less than 10 mm was ignored), α is the seasonal coefficient (0.3101 for warm season from May to September, and 0.3937 for cold season from October to April). Then the daily rainfall erosivity values were accumulated to calculated monthly and annual rainfall erosivity values. The model accuracy has been assessed against rainfall data at 1-min interval using the Nash-Sutcliffe model efficiency coefficient (NSE > 0.80) and ratio of root mean square error to *SD* (RSR < 0.45) (Xie et al., 2016).

This study employed the cloud-based geospatial processing power of GEE for the LANDSAT data processes and implementation of the above calculations. Total 13,801 images from TM (LANDSAT 5–7) and OLI (LANDSAT 8) within the Loess Plateau since 2001 were collected and processed. The spectral bands (visible to SWIR) of the imagery for each overpass, at a ground resolution of 30 m, were radiometrically calibrated and atmospherically corrected to derive the surface reflectance (Yang, Smith, Yu, & Gao, 2011). Automated scripts in GEE were developed to process the time-series LANDSAT data and estimate the FVC and the C-factor values based on Equations (1)–(8).

3.4 | Other RUSLE factors and erosion estimation

This study focused on the C-factor, other RUSLE factors were obtained from the best available datasets for the area. The LS-factor was calculated from the 30 m SRTM DEM based on the methods as described in Yang (2015). The K-factor was obtained from the national Soil Survey database (Shi et al., 2015).

All datasets were converted to raster format and reprojected to the same coordinate system, WGS84 Albers projection (in meters). The datasets were then resampled to a spatial resolution of 100 m which is regarded appropriate for the scale of the study area. Hillslope erosion was then estimated from all these factors and the procedures are illustrated in Figure 2.

3.5 | Validation and accuracy assessment

Ideally, large plot field measurements should be used for validation and accuracy assessment of the estimated C-factor. However, these large plot measurements are rare and difficult to obtain for the entire Loess Plateau. Instead, we chose multiple indirect methods to assess the accuracy of the remotely sensed C-factor by comparing with (a) C-factor values estimated from LANDSAT data (13,801 scenes); (b) C-factor values at Ansai and Wuqi counties (include UBC) within the Loess Plateau from previous studies (e.g., Feng et al., 2017; Zhao et al., 2013); and (c) C-factor values estimated from the field measured FVC at 81 sites along a North–South transect (refer Figure 1) which cover the major land use types (grass, forest, BS, shrubs, desert and cropping areas) and different climate zones. By these means, the C-factor values can be compared and assessed by values, spatial patterns and temporal variations, namely cross validation.

The FVC field measurements followed the star transect method as described in Muir et al. (2011). Each field site, covering an area about 1 ha or a 3 × 3 pixels of LANDSAT imagery, was measured using three transects (100-m tap measures) laid

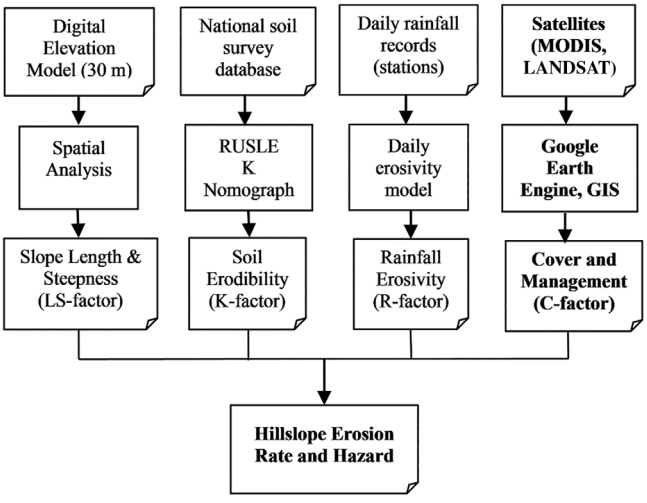

FIGURE 2 The procedures for cover-management factor and hillslope erosion modelling using revised the universal soil loss equation (RUSLE) over the Loess Plateau of China. This study focuses on the cover and management factor (in bold)

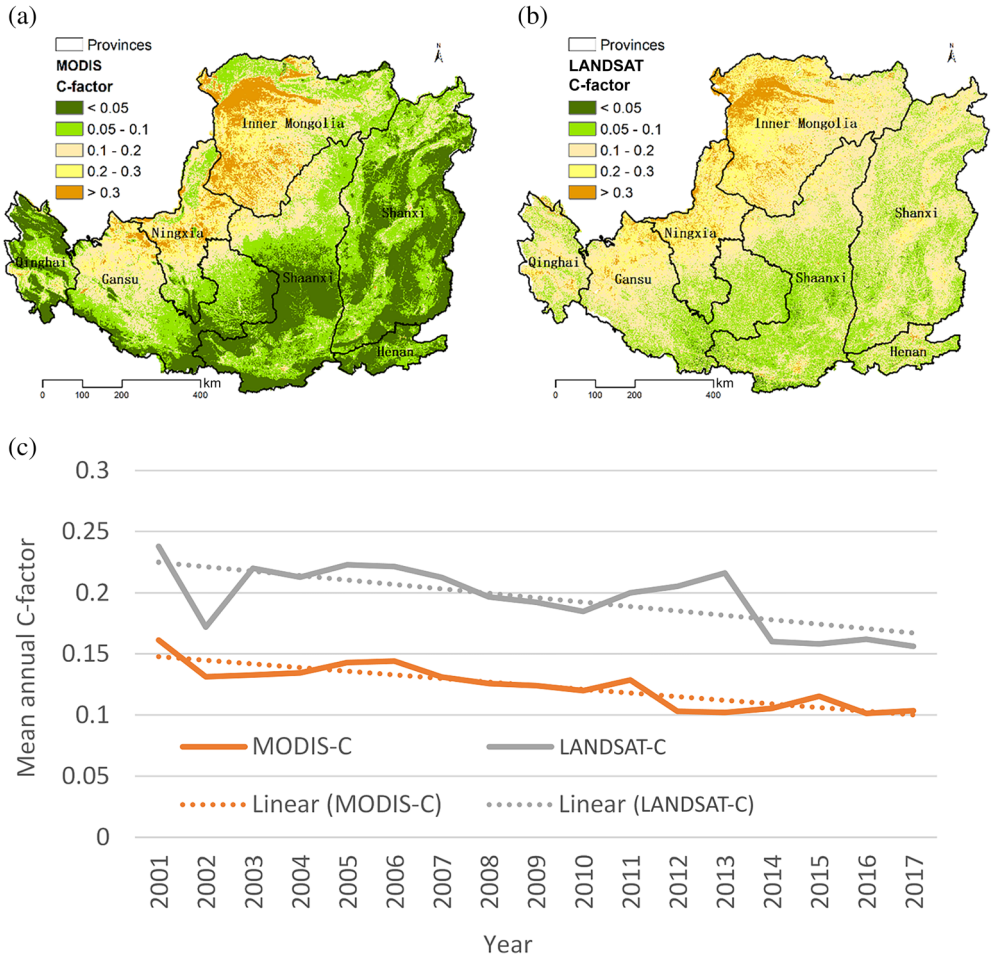

FIGURE 3 Comparison of moderate resolution imaging spectroradiometer (MODIS) derived C-factor with LANDSAT derived C-factor over the Loess Plateau; (a) MODIS derived annual C-factor, (b) LANDSAT derived C-factor, (c) changes of C-factor in period 2001–2017 estimated from MODIS and LANDSAT [Colour figure can be viewed at wileyonlinelibrary.com]

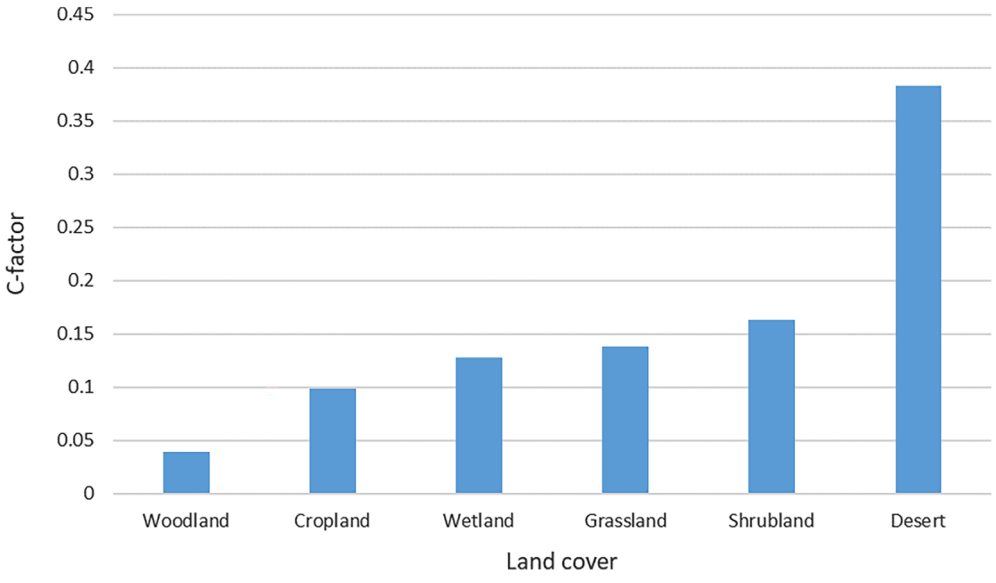

FIGURE 4 Estimated C-factor value at major land cover categories over the Loess Plateau [Colour figure can be viewed at wileyonlinelibrary.com]

out in a star shape, with 100 observations along each (300 observations in total). The first transect runs from north to south, the second from 60 to 240° and the third from 120 to 300°.The measured ground cover categories include BS (crust, disturbed soil, rock, cryptogams), PV (green leaf) and NPV (dry leaf, litter). The selected measurement sites were as large and uniform as possible and covered major land use types and growing seasons.

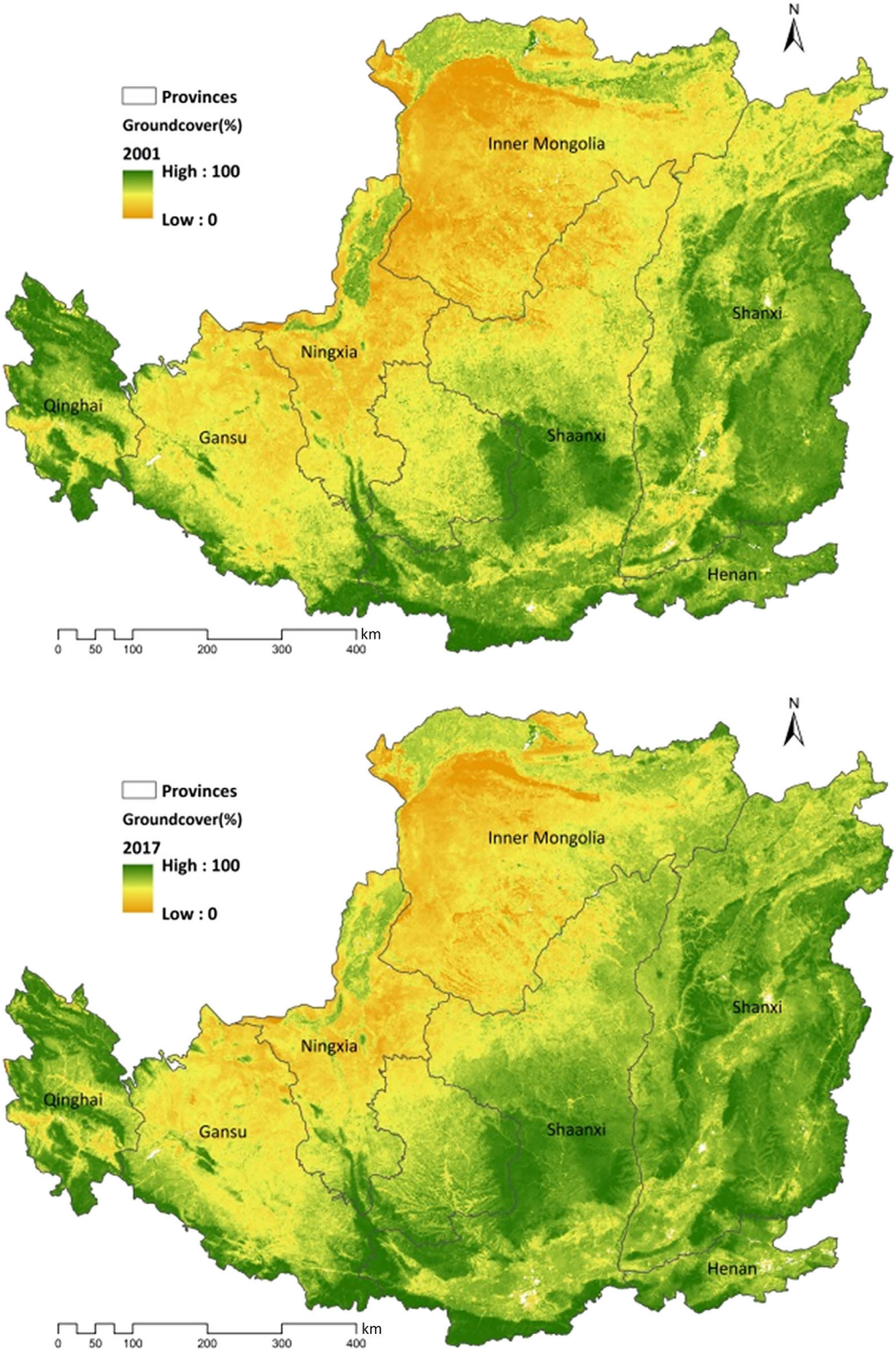

FIGURE 5 Groundcover (%) of the Loess Plateau between 2001 and 2017 [Colour figure can be viewed at wileyonlinelibrary.com]

4 | RESULTS AND DISCUSSION

4.1 | Assessment of FVC derived C-factor

Monthly and annual C-factor values were estimated using MODIS and LANDSAT derived FVC the first time for the entire Loess Plateau of China from 2001 to 2017. Figure 3a,b presents the comparison of MODIS and LANDSAT derived C-factor values based on FVC. Though the absolute values differ, both show similar spatial patterns and a decreasing trend (two trendlines are almost parallel) from 2001 to 2017. The MODIS derived C-factor value is in general systematically lower and smoother (less fluctuation) than LANDSAT-derived C-factor (Figure 3c).

The mean C-factor value derived from the 81 field site measurements is 0.091, the LANDSAT derived mean C-factor value at the same sites is 0.108, while the MODIS derived C-factor value is 0.071. This reveals that MODIS underestimates, while LANDSAT slightly overestimates the C-factor values. These sites are approximately 100 m by 100 m, providing good assessment of satellite estimates, and confirm the magnitude and differences of the C-factor values estimated from different sensors. Though the MODIS-based time series estimations are not absolutely accurate, they are continuous and consistent, thus comparable and useful for the relative change detection of FVC and C-factor values.

The LANDSAT derived annual C-factor values from this study were further compared with a recent study in Ansai County and UBC in central Loess Plateau in which 152 sampling plots and LANDSAT 8 images were used to estimate the C-factor values based on stratified vegetation coverages and remote sensing indices (Feng et al., 2017). They reported a mean annual C-factor value of 0.089 (*SD* = 0.105) in Ansai County. Compared with their results, our estimate of C-factor value (mean = 0.077, *SD* = 0.017) was about 15% lower. One of the reasons to explain why our estimated C-factor values are lower than these studies is that our method considered the TC including PV and NPV and the seasonal variations, while the previous studies mainly focused on PV.

Our estimates of the C-factor values for different land cover types over the Loess Plateau agree in general with many other studies (e.g., Fu et al., 2005; Panagos et al., 2015). Comparison with an earlier study (Fu et al., 2005) over a large catchment (Yanhe Catchment) shows that our estimation of C-factor value is lower at all major land use categories, but in the same order: woodland < cropland < wetland < grassland < shrubland < bareland. This order repeated by using a more recent land cover map derived from the 30 m LANDSAT data (Gong et al., 2013) over the Loess Plateau (Figure 4). However, our study reveals that the C value of cropland is lower compared to some well-known literature (e.g., Panagos et al., 2015). This might be due to the reason that most croplands are at flat areas (e.g., valleys) with irrigation and the area is also getting smaller with improved management due to the GFG Programme policy, thus the vegetation cover is often higher than grassland and shrubland.

4.2 | Changes of FVC, C-factor and erosion over the Loess Plateau

The estimated mean annual vegetation cover (PV + NPV) percent ranges from 56 to 76.8% with a mean of 71.2% across the Loess Plateau for the period 2001–2017 (Figure 5).

The MODIS–FVC shows an obvious trend of increasing, about 20.2% by comparing the beginning and the end of monitoring period (2001–2017). When compared against the baseline period (the mean value of the period 2001–2010), the increase is about 9.4% in the last 3 years, about 11.1% in 2017.

Further examination of the change of fractional cover shows that the increase is mainly due to the increase of the PV component, with the NPV component showing minor change (Figure 6). The BS percentage decreases as the TC increases. The increase of PV might be due to the implementation of the GFG Programme. The GFG program was implemented in 1999, and most plants started to grow rapidly in about 2–3 years (i.e., 2001–2002). This explains the sharp increase of PV from 2001 to 2002 which coincides with the GFG program implementation and agrees well with a recent study on vegetation change over the Loess Plateau (Kong, Miao, Borthwick, Lei, & Li, 2018).

There are great seasonal variations in fractional covers, especially the PV component (Figure 7). PV has the highest cover percentage in summer (July to September) and lowest in winter (January to March), with a fivefold difference. NPV has a strong negative relationship with PV, that is, the highest NPV appears in winter and the lowest in summer, though the variation is less obvious compared to PV.

The changes in FVC resulted in similar spatial and temporal changes in SLR values were relatively low in summer but increased in the months outside of the rainy season due to the decreased TC. The monthly mean SLR values were estimated as: winter (0.143) > spring (0.125) > summer (0.075) > autumn (0.072). Values in winter are twice higher than in summer or autumn, and this reflects the vegetation growing cycle or seasonality. Crops grow rapidly from July to September resulting in high vegetation coverage (or low C-factor)

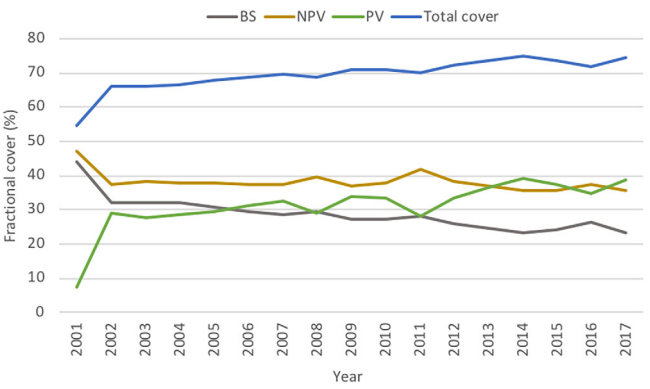

FIGURE 6 Interannual changes of fractional cover (2001–2017) [Colour figure can be viewed at wileyonlinelibrary.com]

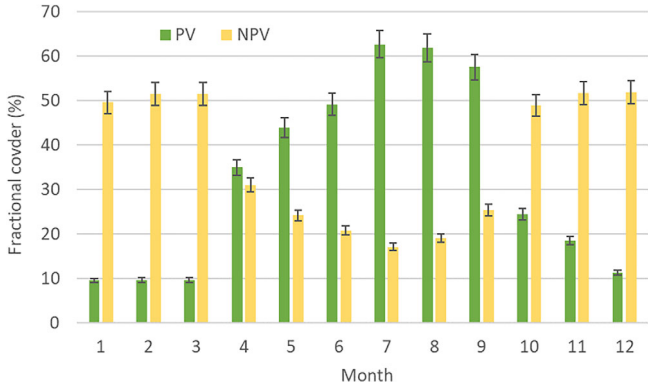

FIGURE 7 The monthly variation of fractional cover [photosynthetic vegetation (PV) and non-PV (NPV)] over the Loess Plateau [Colour figure can be viewed at wileyonlinelibrary.com]

protecting the soils from the direct impact of rainfall splash and detachment (Zhao et al., 2013). However, when the rainfall erosivity ratios were applied to estimate the monthly distribution of C-factor, the mean C-factor values were in the order that summer (0.028) > spring (0.007) > autumn (0.006) > winter (~0), as summer has more erosive rainfall and winter has almost no rain (Figure 8).

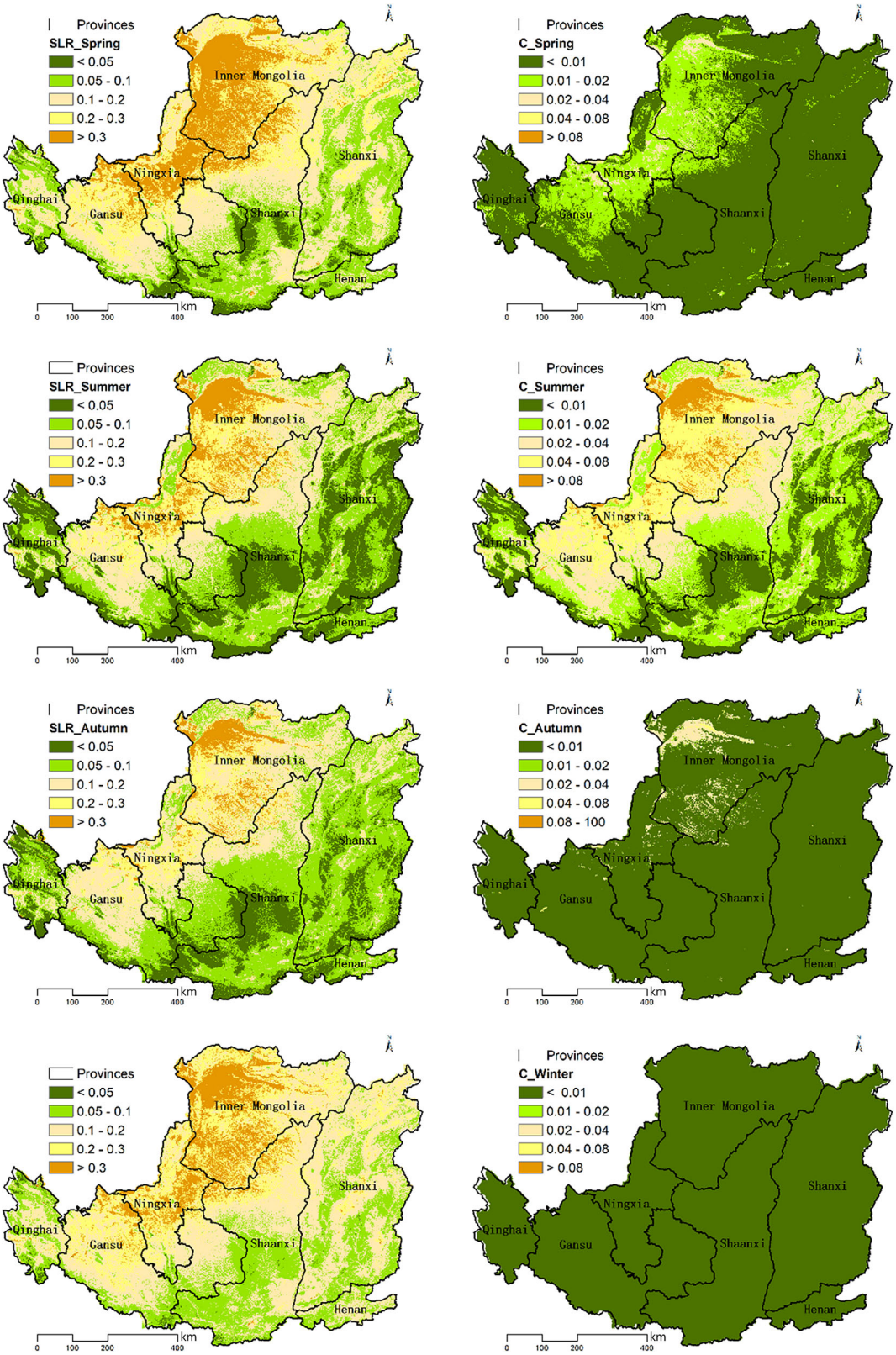

FIGURE 8 Monthly mean soil loss ratio (left) and C-factor (right) in Spring, Summer, Autumn and Winter [Colour figure can be viewed at wileyonlinelibrary.com]

Applying rainfall erosivity ratio in the monthly C-factor calculation resulted in an opposite distribution to the distribution of SLR values as erosive rainfall events are mainly concentrated in summer (Figure 9). Monthly C-factor values range from near zero to 0.024, with a mean of 0.007. The mean C-factor values decreased by about 20% from 2001 to 2017. That means even if all other RUSLE factors remain unchanged, the hillslope erosion rate would decrease by 20% solely due to the change of the C-factor or the increase of vegetation cover (about 20%).

The spatial distribution of the C-factor values contributed to the spatial patterns of erosion risk. Figure 10 shows the RUSLE factors (without P-factor) and the mean annual hillslope erosion across the Loess Plateau. For example, the C-factor values are higher in the north-west part of the Loess Plateau, but the erosion risk is relatively low. This can be explained by the relatively lower LS-factor and R-factor values in that area. In general, our results on the C-factor and erosion risk are in good agreement with that from Sun, Shao, and Liu (2013). On watershed basis, the highest erosion risk areas are Kuyehe River (mean erosion rate 41.6 Mg ha^{-1} yr^{-1}) and Western Weihe (34.2 Mg ha^{-1} yr^{-1}) watershed areas. This was mainly due to the combined effects of vegetation (C) and the terrain (LS) factors. With detailed information on spatial and seasonal variation of the FVC and C-factor as described above, we can not only identify the high erosion risk areas but also the likely timing so that cost-efficient erosion control practices can be applied at specific locations and times.

5 | CONCLUSIONS AND FURTHER DIRECTIONS

We developed and implemented a set of new methodology to estimate and map monthly C-factor for the entire Loess Plateau of China for a continuous period of 17 years (2001–2017) using time-series FVC products derived from MODIS and LANDSAT. We further analysed the spatiotemporal variations of FVC and the C-factor over the Plateau and delineated the potential high erosion risk areas. Our study reveals a significant increase in TC from 56% to 76.8%, with a mean of 71.2%, resulting in 20% decrease in the C-factor and erosion risk during the 17-year period. Our methods have been successfully implemented in GIS and GEE platforms which can be used as efficient tools to continuously and consistently monitor vegetation cover, erosion risk and climate impacts.

This study used the best available global FVC products from 2001 to 2017 to derive long time-series C-factor estimates which can be directly used for soil erosion modelling across the entire Loess Plateau of China. The estimated FVC and monthly C-factor are consistent and continuous across the region, thus useful for analysing the spatial–temporal characteristics of vegetation patterns and their changes anywhere and at any specific time in the past 17 years. Though the absolute values are yet to be further assessed and validated using more field measurements, the time-series outcomes are useful for erosion risk monitoring for the entire area. The C-factor values estimated from MODIS and LANDSAT are in good agreement and consistent, though MODIS underestimates the C-factor values compared to LANDSAT. These time-series products on a monthly interval for 17 years (2001–2017) are, so far, the most detailed (30 or 500 m) and consistent estimates of the C-factor across the Loess Plateau region, thus providing new insights into the changes of fractional cover and the impact on erosion.

Our study reveals the significant increase in vegetation cover (i.e., the green vegetation) and its spatial distribution, these results agree well with the previous studies in the same area. Further, our study identifies the changes of each fractional vegetation component (BS, NPV and PV) on monthly basis for a period of 17 years. This not only contributes significantly to our knowledge base of vegetation changes over the region but also provides a useful tool for assessment of land management policies (e.g., GFG) and best land management practices as the time-series products are directly comparable across space and time.

These time-series FVC and C-factor maps can be used to identify potential high erosion risk areas and spatiotemporal variations, and in

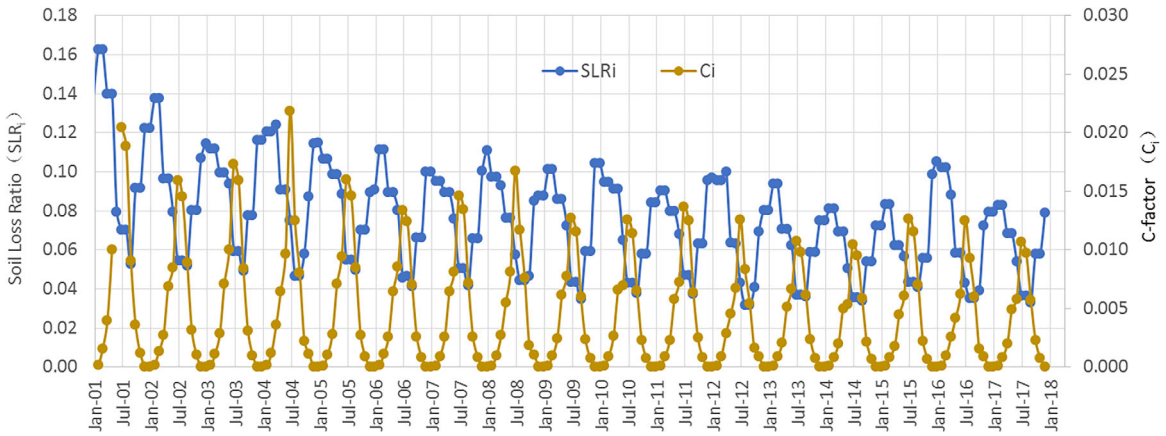

FIGURE 9 Trends and variation of monthly soil loss ratio (SLRi) and C-factor (Ci) in a 17-year period (20012017) over the Loess Plateau [Colour figure can be viewed at wileyonlinelibrary.com]

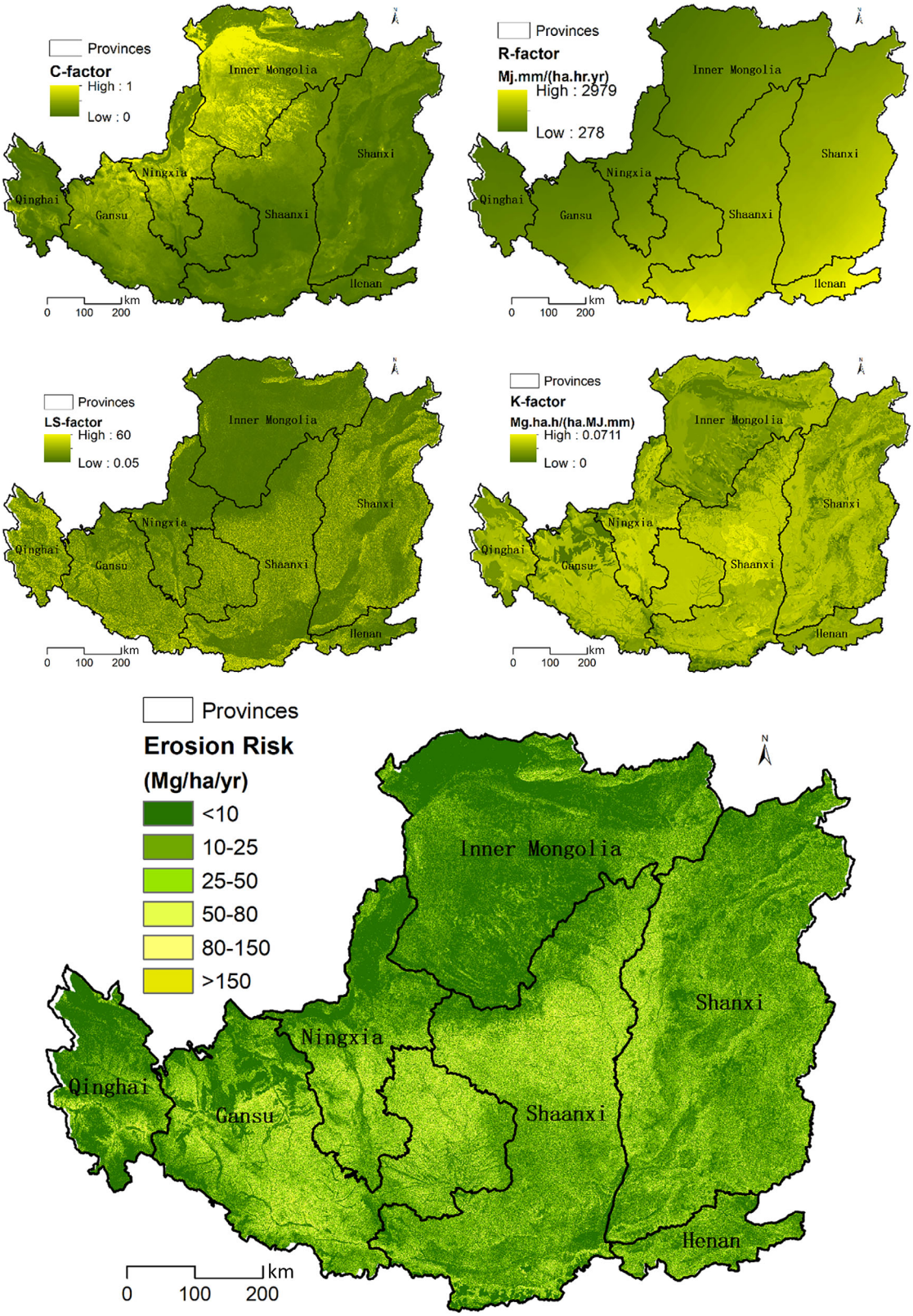

FIGURE 10 The revised universal soil loss equation (RUSLE) factors and the mean annual hillslope erosion risk across the Loess Plateau [Colour figure can be viewed at wileyonlinelibrary.com]

hillslope erosion modelling and other applications. However, the estimated erosion rate resulted from a combined effect of vegetation, climate, topography and soil. Though vegetation cover played a dominant role in interannual changes; whereas, rainfall or storm events might be more influential in seasonal changes. Assessment of the contribution from other factors is yet to be assessed.

Though we used the best available empirical relationships between vegetation cover and the C-factor over the Loess Plateau region, such relationships need to be further assessed and modified when they are used in different regions and land use categories. The relationships also need to be consistent and comparable among different seasons and land use conditions in other regions.

Methodology and automated scripts in GIS and GEE have been developed to process satellite imagery (MODIS and LANDSAT) and map time-series FVC and C-factor across the Loess Plateau. It was the first time the GEE technology has been successfully used for processing the large quantity time-series satellite data in this area. The automated processes in GIS and the GEE platforms are portable and fast so that our methodology can be readily applied to other areas with some minimum modifications.

Given the lack of adequate field measurements for accuracy assessment, previous studies and alternative data sources (e.g., LANDSAT data) provided valuable cross comparisons. Image fusion technologies may further improve the data quality and level of details.

Future study should aim to focus on improving spatial and temporal resolution using newer satellite data or products. More satellite data are now available for FVC estimation at even higher spatial and temporal resolutions such as Sentinel 2/3 and Chinese GF-5/6 satellites. These products will improve the C-factor estimation on the Loess Plateau, assisted with big and fast data processing technologies such as GEE in supercomputers. In the immediate future, we are to blend MODIS and LANDSAT FVC products to improve both spatial and temporal resolutions (30 m at monthly interval) which will have enormous potential in increasing the knowledge regarding changes in cover of different land uses or management practices and the impacts on soil erosion. The detailed and continuous vegetation mapping will provide more comprehensive and accurate information for erosion control and land degradation recovery.

ACKNOWLEDGMENTS

This study was funded by National Natural Science Foundation of China (41877083) and the special funds of scientific research programs of State Key Laboratory of Soil Erosion and Dryland Farming on the Loess Plateau (A314021403-1703). The Laboratory also provided support for using the equipment, assistance in fieldwork and soil plots data. Many research students at Northwest A & F University participated in the field work for vegetation cover measurements and soil data collection. Time-series MODIS fractional cover data were kindly provided by Dr Juan Guerschman from CSIRO Australia. The authors thank researchers on the Loess Plateau for providing their research findings and data for comparison and validation, especially Profs Wenwu Zhao and Yan Zhang. Finally yet importantly, we thank Dr Jonanthan Gray from New South Wales Department of Planning, Industry and Environment, the journal editors and the reviewers for their constructive comments and reviewing of our manuscript.

CONFLICT OF INTEREST

The authors declare no potential conflict of interest.

ORCID

Xihua Yang https://orcid.org/0000-0002-5990-2186
Xiaoping Zhang https://orcid.org/0000-0002-6239-1006
Mingxi Zhang https://orcid.org/0000-0002-5431-9274
Qinggaozi Zhu https://orcid.org/0000-0002-2371-4626

REFERENCES

Benkobi, L., Trlica, M. J., & Smith, J. L. (1994). Evaluation of a refined surface cover subfactor for use in RUSLE. *Journal of Rang Management*, *47*(1), 74–78. https://doi.org/10.2307/4002845

Borrelli, P., Van Oost, K., Meusburger, K., Alewell, C., Lugato, E., & Panagos, P. (2018). A step towards a holistic assessment of soil degradation in Europe: Coupling on-site erosion with sediment transfer and carbon fluxes. *Environmental Research*, *161*, 291–298. https://doi.org/10.1016/j.envres.2017.11.009

Cao, Z., Li, Y., Liu, Y., Chen, Y., & Wang, Y. (2018). When and where did the Loess Plateau turn "green"? Analysis of the tendency and breakpoints of the normalized difference vegetation index. *Land Degradation & Development*, *29*, 162–175. https://doi.org/10.1002/ldr.2852

Chappell, A., Webb, N., Guerschman, J., Thomas, D., Mata, G., Handcock, R., … Butler, H. (2017). Improving ground cover monitoring for wind erosion assessment using MODIS BRDF parameters. *Remote Sensing of Environment*, *204*(11), 756–768. https://doi.org/10.1016/j.rse.2017.09.026

Chen, H., Zhang, X., Abla, M., Lv, D., Yan, R., Ren, Q. F., … Yang, X. (2018). Effects of vegetation and rainfall types on surface runoff and soil erosion on steep slopes on the Loess Plateau, China. *Catena*, *170*, 141–149. https://doi.org/10.1016/j.catena.2018.06.006

De Asis, A. M., & Omasa, K. (2007). Estimation of vegetation parameter for modeling soil erosion using linear spectral mixture analysis of Landsat ETM data. *ISPRS Journal of Photogrammetry and Remote Sensing*, *62*, 309–324. https://doi.org/10.1016/j.isprsjprs.2007.05.013

De Jong, S. M. (1994). Derivation of vegetative variables from a Landsat TM image for modelling soil erosion. *Earth Surface Processes and Landforms*, *19*, 165–178. https://doi.org/10.1002/esp.3290190207

Evans, B. J. K., Antony, J., Guerschman, J. P., Larraondo, P. R., & Richards, C. J. (2017). Geospatial data as a service: The GEOGLAM Rangelands and Pasture Productivity Map Experience American Geophysical Union, Fall Meeting 2017 10–14 December. New Orleans, LA.

Feng, Q., & Zhao, W. W. (2014). The study on cover-management factor in USLE and RUSLE: A review. *Acta Ecologica Sinica*, *34*(16). https://doi.org/10.5846/stxb201306151710

Feng, Q., Zhao, W. W., Ding, J. Y., Fang, X. N., & Zhang, X. (2017). Estimation of the cover and management factor based on stratified coverage and remote sensing indices: A case study in the Loess Plateau of China. *Journal of Soils and Sediments*, *18*(3), 775–790. https://doi.org/10.1007/s11368-017-1783-4

Fu, B. J., Zhao, W. W., Chen, L. D., Zhang, Q. J., Lu, Y. H., Gulinck, H., & Poesen, J. (2005). Assessment of soil erosion at large watershed scale using RUSLE and GIS: A case study in the Loess Plateau of China. *Land Degradation & Development*, *16*, 73–85. https://doi.org/10.1002/ldr.646

Gong, P., Wang, J., Yu, L., Zhao, Y. C., Zhao, Y. Y., Liang, L., et al. (2013). Finer resolution observation and monitoring of global land cover: First mapping results with Landsat TM and ETM+ data. *International Journal of Remote Sensing*, *34*(7), 2607–2654. https://doi.org/10.1080/01431161.2012.748992

Guerschman, J. P., & Hill, M. J. (2018). Calibration and validation of the Australian fractional cover product for MODIS collection 6. *Remote*

Sensing Letters, *9*(7), 696–705. https://doi.org/10.1080/2150704X.2018.1465611

Guerschman, J. P., Hill, M. J., Renzullo, L. J., Barrett, D. J., Marks, A. S., & Botha, E. J. (2009). Estimating fractional cover of photosynthetic vegetation, non-photosynthetic vegetation and bare soil in the Australian tropical savanna region upscaling the EO-1 Hyperion and MODIS sensors. *Remote Sensing of Environment*, *113*, 928–945. https://doi.org/10.1016/j.rse.2009.01.006

Guerschman, J. P., Scarth, P. F., McVicar, T. R., Renzullo, L. J., Malthus, T. J., Stewart, J. B., … Trevithick, R. (2015). Assessing the effects of site heterogeneity and soil properties when unmixing photosynthetic vegetation, non-photosynthetic vegetation and bare soil fractions from Landsat and MODIS data. *Remote Sensing of Environment*, *161*, 12–26. https://doi.org/10.1016/j.rse.2015.01.021

Haboudane, D., Miller, J. R., Pattey, E., Zarco-Tejada, P. J., & Strachan, I. B. (2004). Hyperspectral vegetation indices and novel algorithms for predicting green LAI of crop canopies: Modeling and validation in the context of precision agriculture. *Remote Sensing of Environment*, *90*, 337–352. https://doi.org/10.1016/j.rse.2003.12.013

IUSS Working Group WRB (2014). World Reference Base for Soil Resources 2014. World Soil Resources Report No. 106. FAO, Rome.

Jian, S., Zhao, C., Fang, S., & Kai, Y. (2015). Effects of different vegetation restoration on soil water storage and water balance in the Chinese Loess Plateau. *Agriculture and Forest Meteorology*, *206*, 85–96. https://doi.org/10.1016/j.agrformet.2015.03.009

Jiang, Z. S., Wang, Z. Q., & Liu, Z. (1996). Quantitative study on spatial variation of soil erosion in a small watershed in the loess hilly region. *Journal of Soil Erosion and Soil Conservation*, *2*, 1–9.

Jin, Q. T., Zhang, J. T., Shi, M. C., & Huang, J. X. (2016). Estimating Loess Plateau average annual precipitation with multiple linear regression kriging and geographically weighted regression kriging. *Water*, *8*, 266. https://doi.org/10.3390/w8060266

Ko, D. W., Kim, D., Narantsetseg, A., & Kang, S. (2017). Comparison of field- and satellite-based vegetation cover estimation methods. *Journal of Ecology and Environment*, *41*, 5. https://doi.org/10.1186/s41610-016-0022-z

Kong, D., Miao, C., Borthwick, A. G. L., Lei, X., & Li, H. (2018). Spatiotemporal variations in vegetation cover on the Loess Plateau, China, between 1982 and 2013: Possible causes and potential impacts. *Environmental Science and Pollution Research*, *25*(14), 13633–13644. https://doi.org/10.1007/s11356-018-1480-x

Lal, R. (2001). Soil degradation by erosion. *Land Degradation and Development*, *12*(6), 519–539. https://doi.org/10.1002/ldr.472

Li, Z. Q., & Gao, X. L. (2016). Remote sensing of terrestrial non-photosynthetic vegetation using hyperspectral, multispectral, SAR, and LiDAR data. *Progress in Physical Geography: Earth and Environment*, *40*(2), 276–304. https://doi.org/10.1177/0309133315582005

Marsett, R. C., Qi, J., Heilman, P., Biedenbender, S. H., Watson, M. C., Amer, S., … Marsett, R. (2006). Remote sensing for grassland management in the arid southwest. *Rangeland Ecology and Management*, *59*, 530–540. https://doi.org/10.2111/05-201R.1

McKenzie, N. J., Hairsine, P. B., Gregory, L. J., Austin, J., Baldock, J. A., Webb, M. J., … Thomas, M. (2017). Priorities for improving soil condition across Australia's agricultural landscapes. Report prepared for the Australian Government Department of Agriculture and Water Resources. CSIRO, Australia. Retrieved from https://publications.csiro.au/rpr/pub?pid=csiro:EP177962

Muir, J., Schmidt, M., Tindall, D., Trevithick, R., Scarth, P., & Stewart, J. B. (2011). Field measurement of fractional ground cover: A technical handbook supporting ground cover monitoring for Australia, prepared by the Queensland Department of Environment and Resource Management for the Australian Bureau of Agricultural and Resource Economics and Sciences, Canberra, November.

Panagos, P., Borrelli, P., Meusburger, K., Alewell, C., Lugato, E., & Montanarella, L. (2015). Estimating the soil erosion cover-management factor at the European scale. *Land Use Policy*, *48*, 38–50. https://doi.org/10.1016/j.landusepol.2015.05.021

Puente, C., Olague, G., Smith, S. V., Bullock, S. H., Hinojosa-Corona, A., & González-Botello, M. A. (2011). A genetic programming approach to estimate vegetation cover in the context of soil erosion assessment. *Photogrammetric Engineering & Remote Sensing*, *77*(4), 363–376. https://doi.org/10.14358/PERS.77.4.363

Qi, J., Marsett, R., Heilman, P., Biedenbender, S., Moran, M. S., Goodrich, D. C., & Weltz, M. (2002). RANGES improves satellite based information and land cover assessments in Southwest United States. *Eos, Transactions American Geophysical Union*, *83*(51), 601–606. https://doi.org/10.1029/2002EO000411

Renard, K. G., Foster, G. R., Weesies, G. A., McCool, D. K., & Yoder, D. C. (1997). *Predicting hillslope erosion by water: a guide to conservation planning with the Revised Universal Hillslope Erosion Equation (RUSLE)*, *Agricultural Handbook* (Vol. 703, pp. 1–251). Washington, DC: US Department of Agriculture.

Shi, X. Z., Yu, D. S., Warner, E. D., Pan, X. Z., Petersen, G. W., Gong, Z. G., & Weindorf, D. C. (2015). Soil database of 1:1,000,000 digital soil survey and reference system of the Chinese genetic soil classification system. *Soil Horizons*, *45*(4), 129–136. https://doi.org/10.2136/sh2004.4.0129

Smith, A. M., Hill, M. J., & Zhang, Y. Q. (2015). Estimating ground cover in the mixed prairie grassland of southern Alberta using vegetation indices related to physiological function. *Canadian Journal of Remote Sensing*, *41*(1), 51–66. https://doi.org/10.1080/07038992.2015.1042101

Song, W. J., Mu, X. H., Ruan, G. Y., Gao, Z., Li, L. Y., & Yan, G. J. (2017). Estimating fractional vegetation cover and the vegetation index of bare soil and highly dense vegetation with a physically based method. *International Journal of Applied Earth Observation and Geoinformation*, *58*, 167–176. https://doi.org/10.1016/j.jag.2017.01.015

Sun, W. Y., Shao, Q. Q., & Liu, J. Y. (2013). Soil erosion and its response to the changes of precipitation and vegetation cover on the Loess Plateau. *Journal of Geographical Sciences*, *23*(6), 1091–1106. https://doi.org/10.1007/s11442-013-1065-z

Tanyaş, H., Kolat, Ç., & Süzen, M. L. (2015). A new approach to estimate cover-management factor of RUSLE and validation of RUSLE model in the watershed of Kartalkaya Dam. *Journal of Hydrology*, *528*, 584–598. https://doi.org/10.1016/j.jhydrol.2015.06.048

Vatandaşlar, C., & Yavuz, M. (2017). Modeling cover management factor of RUSLE using very high-resolution satellite imagery in a semiarid watershed. *Environmental Earth Sciences*, *76*, 267. https://doi.org/10.1007/s12665-017-6388-0

Vrieling, A. (2006). Satellite remote sensing for water erosion assessment. A Review. *Catena*, *65*, 2–18. https://doi.org/10.1016/j.catena.2005.10.005

Wang, G., Wente, S., Gertner, G. Z., & Anderson, A. (2010). Improvement in mapping vegetation cover factor for the universal soil loss equation by geostatistical methods with Landsat thematic mapper images. *International Journal of Remote Sensing*, *23*(18), 3649–3667. https://doi.org/10.1080/01431160110114538

Wischmeier, W. H., & Smith, D. D. (1978). *Predicting rainfall erosion losses, a guide to conservation planning. Agricultural handbook* (Vol. 537, p. 58). Washington, DC: US Department of Agriculture.

Xie, Y., Yin, S. Q., Liu, B. Y., Nearing, M. A., & Zhao, Y. (2016). Models for estimating daily rainfall erosivity in China. *Journal of Hydrology*, *535*, 547–558. https://doi.org/10.1016/j.jhydrol.2016.02.020

Yang, Q., & Yuan, B. (1991). *The natural environment and evolution of the Loess Plateau*. Beijing: Science Press.

Yang, X. (2014). Deriving RUSLE cover factor from time-series fractional vegetation cover for hillslope erosion risk monitoring in New South Wales. *Soil Research*, *52*, 253–261. https://doi.org/10.1071/SR13297

Yang, X. (2015). Digital mapping of RUSLE slope length and steepness factor across New South Wales. *Soil Research*, *53*, 216–225. https://doi.org/10.1071/SR14208

Yang, X., Smith, P., Yu, T., & Gao, H. (2011). Estimating evapotranspiration from terrestrial groundwater dependant ecosystems using Landsat images. *International Journal of Digital Earth*, *4*(2), 154–170. https://doi.org/10.1080/17538947.2010.491561

Zhang, C. S., Hu, Y., & Shi, X. L. (2016). Analysis of spatial-temporal evolution of vegetation cover in loess plateau in recent 33 years based on AVHRR NDVI and MODIS NDVI. *Journal of Applied Sciences (in Chinese with English Abstract)*, *34*(6), 702–712. https://doi.org/10.3969/j.issn.0255-8297.2016.06.006

Zhang, X., Lin, P. F., Chen, H., Yan, R., Liu, E. J., Abla, M., … Li, Z. G. (2018). Understanding land use/cover change impacts on runoff and -sediment load at flood events behavior under land cover change in a catchment on the Loess Plateau, China. *Hydrological Processes*, *32*(4), 576–589. https://doi.org/10.1002/hyp.11444

Zhang, Y., & Smith, A. M. (2010). Estimation of percent ground cover in grasslands from hyperspectral and multi-angle remote sensing imagery. In: Proceedings of Prairie Summit—31st Canadian Remote Sensing Symposium. June 1–5. Regina, Saskatchewan, Canada. 345–348.

Zhang, Y., Yuan, J., & Liu, B. (2002). Advance in researches on vegetation cover and management factor in the soil erosion prediction model. *Chinese Journal of Applied Ecology*, *13*(8), 1033–1036.

Zhao, W. W., Fu, B. J., & Chen, L. D. (2012). A comparison between soil loss evaluation index and the C-factor of RUSLE: A case study in the Loess Plateau of China. *Hydrology and Earth System Sciences*, *16*, 2739–2748. https://doi.org/10.5194/hess-16-2739-2012

Zhao, W. W., Fu, B. J., & Qiu, Y. (2013). An upscaling method for cover-management factor and its application in the Loess Plateau of China. *International Journal of Environmental Research and Public Health*, *10*, 4752–4766. https://doi.org/10.3390/ijerph10104752

How to cite this article: Yang X, Zhang X, Lv D, et al. Remote sensing estimation of the soil erosion cover-management factor for China's Loess Plateau. *Land Degrad Dev*. 2020;31: 1942–1955. https://doi.org/10.1002/ldr.3577